

Operational-space wrench and acceleration capability analysis for multi-link cable-driven robots

[XinJun SHENG](#), [Lei TANG](#), [XinJia HUANG](#), [LiMin ZHU](#), [XiangYang ZHU](#) and [GuoYing GU](#)

Citation: [SCIENCE CHINA Technological Sciences](#); doi: 10.1007/s11431-019-1525-0

View online: <http://engine.scichina.com/doi/10.1007/s11431-019-1525-0>

Published by the [Science China Press](#)

Articles you may be interested in

[Confined spaces path following for cable-driven snake robots with prediction lookup and interpolation algorithms](#)

SCIENCE CHINA Technological Sciences **63**, 255 (2020);

[Effect of seed electron injection on chorus-driven acceleration of radiation belt electrons](#)

SCIENCE CHINA Technological Sciences **56**, 492 (2013);

[Two-stage acceleration of interstellar ions driven by high-energy lepton plasma flows](#)

SCIENCE CHINA Physics, Mechanics & Astronomy **58**, 105201 (2015);

[Task space control of free-floating space robots using constrained adaptive RBF-NTSM](#)

SCIENCE CHINA Technological Sciences **57**, 828 (2014);

[Synergy methodology for multi-objective operational control of reservoirs in Yellow River basin](#)

Science in China Series E-Technological Sciences **47**, 212 (2004);

Operational-space wrench and acceleration capability analysis for multi-link cable-driven robots

SHENG XinJun^{1,2†}, TANG Lei^{1,2†}, HUANG XinJia^{1,2}, ZHU LiMin²,
ZHU XiangYang^{1,2} & GU GuoYing^{1,2*}

¹ Robotics Institute, School of Mechanical Engineering, Shanghai Jiao Tong University, Shanghai 200240, China;

² State Key Laboratory of Mechanical System and Vibration, Shanghai Jiao Tong University, Shanghai 200240, China

Received October 9, 2019; accepted January 13, 2020; published online April 20, 2020

Multi-link cable-driven robots (MCDRs) have potential advantages in confined spaces exploration because of their redundancy and flexibility. Operational space wrench and acceleration capability analysis of MCDRs is important for their design, manipulability optimization, and motion planning. However, existing works mainly focus on capability analysis in the joint space. In this paper, we present a zonotope-based iterative method and a simplified capability zonotope to analyze the operational-space wrench and acceleration capability of MCDRs. In the iterative method, the capability generated by some cables can be iteratively added to the initial capability zonotope based on the Minkowski sum. In the simplified zonotope capability representation, a threshold is put forward to reduce redundant vertices and faces with little volume loss. Finally, simulations on a 24 DOFs MCDR are performed to verify the effectiveness of the developed method. The results demonstrate that our iterative algorithm can easily generate the capability zonotope with a few MB ROM, while traditional operational wrench capability evaluation without our iterative algorithm needs 18432 GB ROM. Furthermore, our simplified representation reduces the vertices and faces from 1260 and 2516 to 88 and 172, respectively, but with only 3.3% volume loss, which decreases the constraints of the robot and is conducive to manipulability optimization and motion planning.

multi-link cable-driven robots, operational space, capability analysis, zonotope

Citation: Sheng X J, Tang L, Huang X J, et al. Operational-space wrench and acceleration capability analysis for multi-link cable-driven robots. *Sci China Tech Sci*, 2020, 63, <https://doi.org/10.1007/s11431-019-1525-0>

1 Introduction

Cable-driven robots are driven by cables attached to them instead of rigid-linked mechanism, which leads to light-weight structures and flexible motions for confined space exploration [1–3]. Based on the differences of mechanical structures, the cable-driven robots can be roughly classified into two types: cable-driven parallel robots (CDPRs) [4–6] and multi-link cable-driven robots (MCDRs) [7,8]. In

CDPRs, the cables are, respectively, connected to the moving platform and base, which results in large workspace [9], easiness of reconfiguration [10], and suitable for load lift [11], civil construction [12] and motion simulators [13]. Alternatively, MCDRs consist of several CDPRs with joints in a serial way. With the increasing number of CDPRs, MCDRs exhibit the shape of some creatures like snakes and elephant trunks, thus, MCDRs, also termed as snake-like robots, are flexible and promising for inspection and maintenance in intricate industrial environments [1,3,14,15] and minimally invasive surgery [16].

†These authors contributed equally to this work.

*Corresponding author (email: guguoying@sjtu.edu.cn)

Most tasks are performed by the end effector of MCDRs in the operational space, which makes the operational space wrench and acceleration capability analysis important. However, existing capability analysis works mainly focus on CDRs by the prevailing zonotope-based method [17–21]. The zonotope-based method originates from the manipulability ellipsoid proposed by Yoshikawa [22]. The ellipsoid is quite suitable for the capability analysis of rigid-link robots, however, it is generally difficult to be used for cable-driven robots due to the fact that the actuation spaces of cable-driven robots should be always at the pulling states, and each actuation unit usually has different upper and lower bounds. To address these problems, a zonotope-based method has been proposed to generate capability zonotope of CDRs by projecting the cable forces hypercube. Traditional zonotope-based method generally projects the cable force hypercube by dynamics relationships. Then, the vertices of the cable force hypercube are candidates for the corresponding capability zonotope. Afterwards, the convhulln algorithm is developed to select actual vertices of capability zonotope from the candidate set. Thus, the vertices set of capability zonotope is a subset of the vertices of the projected force hypercube. In this sense, capability zonotopes can be numerically found by using the projection of the force hypercube vertices. For instance, Yang's Group [17] presented the force closure workspace analysis of CDRs in terms of the zonotope. Gosselin's Group [18] illustrated three different presentations of available wrench set of cable-driven robots with zonotope. Eden et al. [19] presented capability metrics for CDRs with the help of capability zonotope. Ebert-Uphoff's Group [20] developed an analytical method for generating wrench feasible workspace of CDRs with the relationships between the required and available wrench convex sets. Hassan and Khajepour [21] analyzed the cable force of CDRs by the intersection between the convex set of the null space of Jacobian matrix and available cable force.

Recently, some works have been reported on MCDRs in joint spaces. Mustafa and Agrawal [23] employed reciprocal screw theory on the force-closure analysis of MCDRs. They determined the joint torques and cable tensions for external wrenches. Rezazadeh and Behzadipour [24] extended the null space analysis to the wrench feasible analysis of MCDRs by utilizing the redundancy of cable force. However, operational wrench and acceleration capability analysis of MCDRs is quite challenge because of the hyper-redundancy and multilayer relationships of cables, joints and end effector of MCDRs. Specifically, hyper-redundant actuators of MCDRs make their operational wrench capability analysis consumes large number of memory. There are 2^m vertices for m -cables MCDRs. Thus, the convhulln algorithm should deal with 2^m candidate vertices. With the increasing cables, the set of combination of cable force bound becomes huge. For instance, there are 2^{36} vertices in the cable force

hypercube of the 24 DOFs MCDRs, and the computer needs 18432 GB memory to deal with such massive points, which is usually infeasible for implementation.

In summary, traditional capability analysis of rigid-link robots deals with the operational space capability problem ignoring the actual joint space actuation constraints, and the capability analysis for CDRs only derives in the joint space with cable actuation capability strictly considered. However, the traditional capability analysis methods employed by rigid-link robots and CDRs are not suitable for operational capability analysis of MCDRs due to their actuation constraints and hyper-redundancy. With the increase of the cables, the number of vertices to be processed grows exponentially, which can be computationally infeasible. Until now, the operational space capability analysis of MCDRs has not been achieved.

This work is, therefore, motivated and contributed to develop an efficient zonotope-based operational wrench and acceleration capability analysis method for MCDRs. An alternative algorithm is developed to iteratively generate the zonotope by the Minkowski sum. Instead of generating the zonotope by all cable forces, we can add the capability generated by some cables to the capability zonotope generated by others. Thus, some initial cable forces can be randomly chosen to generate the initial capability zonotope, and iteratively add the capability of other cables by the Minkowski sum. Another problem for the capability zonotope of MCDRs is that large numbers of redundant vertices and faces are generated due to the hyper-redundancy of actuators, which makes the computation cumbersome of post-processing like manipulability optimization and motion planning. We find that many redundant vertices and faces have little contribution to the volume of zonotope. Therefore, a simplified zonotope capability representation is developed to reduce vertices and faces with little volume loss. Finally, radius of capability ball and distance of capability direction are developed based on the capability zonotope to evaluate the maximum payload of MCDRs at a given reference position and direction, respectively. Simulations results on a 24 DOFs MCDR with 36 driven cables verify the memory and time efficiency and effectiveness of the presented method.

The rest of this paper is organized as follows. Section 2 introduces the capability analysis problem base on zonotope and the dynamics model of MCDRs. Section 3 presents the iterative method to calculate the operational wrench and acceleration zonotope of MCDRs. The simplified zonotope representation of capability is also presented in this section. In Section 4, simulations on a 24 DOFs MCDR are performed to verify the effectiveness of the presented method. Two capability metric indexes based on the operational capability zonotope are also presented in this section. Section 5 concludes this paper.

2 Wrench and acceleration capability analysis of MCDRs

2.1 Zonotope representation of available capability set

Zonotope is a special class of convex polytopes, which can be described by the vector sum of a finite number of closed line segments [25] or the Minkowski sum of some line segments [26]. The mathematic presentation of available capability set is related to the definition of zonotope [18], which can exactly represent the set of all the possible acceleration (acceleration zonotope) or wrench (wrench zonotope) generated by the cable forces. In this work, the expressions of capability sets are derived from the dynamic model in Section 2, which satisfy the definition of zonotope. The capability (acceleration or wrench) set of MCDRs \mathbf{A} generated by the given cable forces can be described by

$$\mathbf{A} = \mathbf{P}\mathbf{f} + \mathbf{Offset} \quad 0 \leq \mathbf{f}_{\min} \leq \mathbf{f} \leq \mathbf{f}_{\max} \quad (1)$$

where \mathbf{P} is the projection matrix from the available cable force set to capability set, and \mathbf{Offset} is the translation vector between two projection sets. The cable force vector is \mathbf{f} , and cable force constraint bounds are \mathbf{f}_{\min} and \mathbf{f}_{\max} , respectively. Cables can only pull, thus, \mathbf{f}_{\min} is positive to overcome slack.

The presentation in eq. (1) is corresponded to definition of a zonotope. The projection matrix \mathbf{P} defines the shape of the zonotope, and the translation vector \mathbf{Offset} determines its position. \mathbf{P} and \mathbf{Offset} can be derived from the dynamics model of MCDRs. The convhulln algorithm provided by MATLAB platform will give the capability zonotope in the form of eq. (2) according to the force hypercube vertices, \mathbf{P} and \mathbf{Offset} .

$$\mathbf{A}_c \mathbf{t} \leq \mathbf{b}, \quad (2)$$

where \mathbf{A}_c and \mathbf{b} are the matrix and vector for the combinations of constraint inequalities. The element \mathbf{t} in capability set should satisfy the constraints in eq. (2), which is the mathematic presentation for capability set.

2.2 Dynamic model of MCDRs

Dynamics of MCDRs is the base of its capability analysis, which has been extensively studied by many researches [27–30]. The dynamics between actuation and joint spaces of n -DOFs MCDRs actuated by m cables can be denoted in eq. (3).

$$\mathbf{M}(\mathbf{q})\ddot{\mathbf{q}} + \mathbf{C}(\mathbf{q}, \dot{\mathbf{q}}) + \mathbf{G}(\mathbf{q}) + \mathbf{W}_{\text{ext}} = -\mathbf{L}^T(\mathbf{q})\mathbf{f}, \quad 0 \leq \mathbf{f}_{\min} \leq \mathbf{f} \leq \mathbf{f}_{\max} \quad (3)$$

where \mathbf{q} is the generalized coordinates of joint space, $\mathbf{f} = [\mathbf{f}_1 \dots \mathbf{f}_m]^T \in \mathbf{R}^m$ is the cable force vector, $\mathbf{M} \in \mathbf{R}^{(n \times n)}$ is the symmetric positive definite mass-inertia matrix, $\mathbf{C} \in \mathbf{R}^n$ is the Coriolis/centrifugal force vector, $\mathbf{G} \in \mathbf{R}^n$ is the gravitational force vector, $\mathbf{W}_{\text{ext}} \in \mathbf{R}^n$ is the joint wrench vector exerted by external wrench and $\mathbf{L} \in \mathbf{R}^{(m \times n)}$ is the cable Jacobian matrix from

the actuation space to the joint space.

The dynamics between joint and operational spaces of n -DOFs MCDRs actuated by m cables can be denoted in eq. (4).

$$\mathbf{M}_O(\mathbf{x})\ddot{\mathbf{x}} + \mathbf{C}_O(\mathbf{x}, \dot{\mathbf{x}}) + \mathbf{G}_O(\mathbf{x}) + \mathbf{W}_{\text{ext}_O} = \mathbf{F}, \quad (4)$$

where $\mathbf{x} \in \mathbf{R}^6$ is the generalized coordinates of operational space, $\mathbf{M}_O \in \mathbf{R}^{(6 \times 6)}$, $\mathbf{C}_O \in \mathbf{R}^6$, $\mathbf{G}_O \in \mathbf{R}^6$ are the symmetric positive definite mass-inertia matrix, Coriolis/centrifugal force vector, gravitational force vector in the operational space, respectively. $\mathbf{W}_{\text{ext}_O} \in \mathbf{R}^6$ is the wrench vector exerted by external wrench. $\mathbf{J} \in \mathbf{R}^{(6 \times n)}$ is the joint Jacobian matrix from the joint space to the operational space. $\mathbf{F} \in \mathbf{R}^6$ is the operational space wrench. The relationships between the parameters of the two dynamics equations are shown in eq. (5).

$$\begin{aligned} \mathbf{M}_O &= (\mathbf{J}\mathbf{M}^{-1}\mathbf{J}^T)^{-1}, \\ \mathbf{C}_O &= \mathbf{M}_O\mathbf{J}\mathbf{M}^{-1}\mathbf{C}\dot{\mathbf{q}} - \mathbf{M}_O\dot{\mathbf{J}}\dot{\mathbf{q}}, \\ \mathbf{G}_O &= \mathbf{M}_O\mathbf{J}\mathbf{M}^{-1}\mathbf{G}, \\ \mathbf{W}_{\text{ext}_O} &= \mathbf{M}_O\mathbf{J}\mathbf{M}^{-1}\mathbf{W}_{\text{ext}}. \end{aligned} \quad (5)$$

The joint torque $\boldsymbol{\tau}$ generated by cable forces can be denoted by eq. (6), and the relationship between the joint torque and the operational space wrench is presented in eq. (7). The relationship of eq. (8) can be obtained according to eqs. (6) and (7)

$$\boldsymbol{\tau} = -\mathbf{L}^T(\mathbf{q})\mathbf{f}, \quad (6)$$

$$\mathbf{J}^T(\mathbf{q})\mathbf{F} = \boldsymbol{\tau}, \quad (7)$$

$$\mathbf{J}^T(\mathbf{q})\mathbf{F} = -\mathbf{L}^T(\mathbf{q})\mathbf{f}. \quad (8)$$

2.3 Acceleration capability

Given a pose and a set of available cable forces, the acceleration set that the joint can produce is defined as the available joint acceleration that the MCDR can produce. The available joint acceleration set can be expressed as eq. (9) by using eq. (3).

$$\begin{aligned} \mathbf{a}_j &= -\mathbf{M}^{-1}\mathbf{L}^T\mathbf{f} - \mathbf{M}^{-1}(\mathbf{C} + \mathbf{G} + \mathbf{W}_{\text{ext}}), \\ 0 &\leq \mathbf{f}_{\min} \leq \mathbf{f} \leq \mathbf{f}_{\max} \end{aligned} \quad (9)$$

The acceleration set that the end effector can produce is defined as the available operational acceleration that the MCDRs can produce. Given a pose and the available cable force set, the available operational acceleration set can be expressed as eq. (10) according to eqs. (4), (5) and (8).

$$\begin{aligned} \mathbf{a}_O &= -\mathbf{J}\mathbf{M}^{-1}\mathbf{L}^T\mathbf{f} - \mathbf{J}\mathbf{M}^{-1}(\mathbf{C} + \mathbf{G} + \mathbf{W}_{\text{ext}}) + \dot{\mathbf{J}}\dot{\mathbf{q}}, \\ 0 &\leq \mathbf{f}_{\min} \leq \mathbf{f} \leq \mathbf{f}_{\max} \end{aligned} \quad (10)$$

2.4 Wrench capability

The available wrench set that the joint can produce is defined

as the set of joint space wrenches that the MCDRs can produce. With a given pose and a set of available cable forces, the available joint wrench set can be expressed as eq. (11) by using eq. (3).

$$\begin{aligned} \mathbf{w}_j &= -\mathbf{L}^T \mathbf{f} - \mathbf{C} - \mathbf{G} - \mathbf{W}_{\text{ext}}, \\ 0 &\leq \mathbf{f}_{\min} \leq \mathbf{f} \leq \mathbf{f}_{\max} \end{aligned} \quad (11)$$

The available wrench set that the end effector can produce is defined as the set of operational space wrenches that the MCDRs can produce. We can see that the cable force \mathbf{f} and the operational space wrench \mathbf{F} have the relationship as shown in eq. (8). However, due to the redundancy of MCDRs, the Jacobian matrix \mathbf{J} is non-square and not invertible. Thus, unlike the available joint acceleration, wrench and operational acceleration, there is no explicit projection equation from cable forces to the operational wrench. To obtain the available operational space wrench, we propose three methods in this section. The first two methods are based on the available operational acceleration zonotope. In method 3, the explicit projection equation from cable forces to the operational wrench is derived.

(1) Method 1

Assuming the mathematic presentation of available operational acceleration zonotope generated by eq. (10) is denoted as eq. (12).

$$\mathbf{A}_{\text{ao}} \ddot{\mathbf{x}} \leq \mathbf{b}_{\text{ao}}. \quad (12)$$

Combining eqs. (4), (5) and (12), the constraints for available operational wrench can be denoted in eq. (13).

$$\mathbf{A}_{\text{ao}} \mathbf{J} \mathbf{M}^{-1} \mathbf{J}^T \mathbf{F} \leq \mathbf{b}_{\text{ao}} + \mathbf{A}_{\text{ao}} \mathbf{J} \mathbf{M}^{-1} \mathbf{J}^T (\mathbf{C}_O + \mathbf{G}_O + \mathbf{W}_{\text{ext}}). \quad (13)$$

Thus, the zonotope presentation of operational available wrench can be rearranged as eq. (14).

$$\begin{aligned} \mathbf{A}_F \mathbf{F} &\leq \mathbf{b}_F, \\ \mathbf{A}_F &= \mathbf{A}_{\text{ao}} \mathbf{J} \mathbf{M}^{-1} \mathbf{J}^T, \\ \mathbf{b}_F &= \mathbf{b}_{\text{ao}} + \mathbf{A}_{\text{ao}} \mathbf{J} \mathbf{M}^{-1} \mathbf{J}^T (\mathbf{C}_O + \mathbf{G}_O + \mathbf{W}_{\text{ext}}). \end{aligned} \quad (14)$$

(2) Method 2

Method 1 can get the mathematic presentation of the available operational wrench. However, the vertices of the zonotope cannot be obtained. In order to get the mathematic presentation of available operational wrench zonotope together with its vertices information, we utilize the vertices set of the available operational acceleration zonotope instead of its mathematic presentation. There is explicit projection relationship from operational acceleration to operation wrench, which has been expressed in eq. (4). The vertices of the available operational acceleration zonotope (\mathbf{V}_{ao}) can be acquired from eq. (10). According to the zonotope presentation theory introduced before, we can get the zonotope of available operational wrench by the convhulln algorithm with \mathbf{V}_{ao} , \mathbf{P} and **Offset** in eq. (15).

$$\begin{aligned} \mathbf{P} &= \mathbf{M}_O, \\ \mathbf{Offset} &= \mathbf{C}_O + \mathbf{G}_O + \mathbf{W}_{\text{ext}}. \end{aligned} \quad (15)$$

(3) Method 3

In this method, we strive to find the explicit projection relationship from cable force to operational wrench. Firstly, combining eqs. (4), (5) and (8), the projection relationship from cable force to operational acceleration can be derived, which is shown in eq. (10). Secondly, the relationship between operational force and operational acceleration can also be found by combining eqs. (4) and (5), which is denoted in eq. (16).

$$\begin{aligned} \mathbf{a}_O &= \mathbf{J} \mathbf{M}^{-1} \mathbf{J}^T \mathbf{F} - \mathbf{J} \mathbf{M}^{-1} (\mathbf{C} + \mathbf{G} + \mathbf{W}_{\text{ext}}) + \dot{\mathbf{J}} \dot{\mathbf{q}}, \\ 0 &\leq \mathbf{f}_{\min} \leq \mathbf{f} \leq \mathbf{f}_{\max} \end{aligned} \quad (16)$$

Comparing eq. (16) with eq. (10), the relationship between cable force and operational wrench can be found, which is shown in eq. (17). It should be noticed that the matrix in front of $\mathbf{F}(\mathbf{J} \mathbf{M}^{-1} \mathbf{J}^T)$ is the inverse of the operational symmetric positive definite mass-inertia matrix, which means the matrix $\mathbf{J} \mathbf{M}^{-1} \mathbf{J}^T$ is invertible. In this sense, we can get the available operational wrench set as shown in eq. (18).

$$\mathbf{J} \mathbf{M}^{-1} \mathbf{J}^T \mathbf{F} = -\mathbf{J} \mathbf{M}^{-1} \mathbf{L}^T \mathbf{f}, \quad (17)$$

$$\begin{aligned} \mathbf{w}_O &= -(\mathbf{J} \mathbf{M}^{-1} \mathbf{J}^T)^{-1} \mathbf{J} \mathbf{M}^{-1} \mathbf{L}^T \mathbf{f}, \\ 0 &\leq \mathbf{f}_{\min} \leq \mathbf{f} \leq \mathbf{f}_{\max} \end{aligned} \quad (18)$$

In summary, the first two methods both obtain the operational wrench capability from the acceleration zonotope. The differences are that the method 1 derives the operational wrench capability from the formulation for the possible wrench, while the method 2 depends on the vertices information of acceleration zonotope. By contrast, the method 3 directly derives the explicit projection of wrench capability zonotope by the relation between the cable forces and the wrench.

3 Iterative method to calculate the zonotope of operational wrench and acceleration of MCDRs

As illustrated in the introduction, traditional zonotope-based method often wholly projects the cable force hypercube by dynamics relationships and cannot calculate capability of hyper-redundant cable-driven robots. For instance, there are 2^{36} vertices in the cable force hypercube of the 24 DOFs MCDRs, and the computer needs 18432 GB memory to deal with such massive points, which is usually infeasible for implementation. Fortunately, we find the zonotope can be generated by the Minkowski sum iteratively. In geometry, the Minkowski sum of two sets of vectors \mathbf{A} and \mathbf{B} is formed by adding one vector in \mathbf{A} to another vector in \mathbf{B} . If \mathbf{A} and \mathbf{B} represent two capability zonotopes generated from different sets of cables, the Minkowski sum of them will form a new

zonotopes containing the operational capability of all these cables. Thus, to solve the computation challenge, we proposed an iterative method for the formulation of capability zonotope based on the Minkowski sum. Minkowski sum is defined by eq. (19), in which \mathbf{B} and \mathbf{C} are the vertices sets of zonotopes.

$$\mathbf{B} \oplus \mathbf{C} = \{\mathbf{b} \oplus \mathbf{c} \mid \mathbf{b} \in \mathbf{B}, \mathbf{c} \in \mathbf{C}\}. \quad (19)$$

In this sense, we can randomly choose some initial cable forces to generate the base capability zonotope, and iteratively add the capability of other cables to the base zonotope by the Minkowski sum. The iterative method presented in this work can generate the capability zonotope effectively and efficiently. In this method, I_c is the initial number of cables, which is used to generate the original zonotope. S_c is the number of cables added to the original zonotope each step. Details of the iterative method are presented as follows, and the flowchart of the presented method is shown in Figure 1.

Inputs: projection matrix \mathbf{P} , translation vector **Offset**, cable force constraint bounds \mathbf{f}_{\min} and \mathbf{f}_{\max} .

Outputs: the matrix and vector \mathbf{A}_c and \mathbf{b} for the combinations of constraint equations of the capability zonotope.

• **Step 1:** The number of cables to form zonotope is determined as N_c . Choose $N_c=I_c$ cables and use $\mathbf{P}(N_c)$, $\mathbf{f}_{\min}(N_c)$, $\mathbf{f}_{\max}(N_c)$, to generate base zonotope with its vertices set recorded as $\mathbf{V}(I_c)$.

• **Step 2:** Define a bool variable, if the base zonotope generates successfully, set conflag=1, and go to step 3; else conflag=0, and go to step 4.

• **Step 3:** Choose $N_c=S_c$ cables from the remaining to generate the capability zonotope with $\mathbf{P}(S_c)$, $\mathbf{f}_{\min}(S_c)$, $\mathbf{f}_{\max}(S_c)$ with its vertices set recorded as $\mathbf{V}(S_c)$. If conflag=1, go to step 5; else go to step 4.

• **Step 4:** $N_c=N_c+1$, if $N_c \leq 10$ and $\mathbf{P}(N_c)$ is full rank, go to step 1, else exit the loop.

• **Step 5:** Sum $\mathbf{V}(I_c)$ with $\mathbf{V}(S_c)$ by the Minkowski algorithm to get the candidate vertices set $\mathbf{C}=\mathbf{V}(I_c) \oplus \mathbf{V}(S_c)$, and generate zonotope with \mathbf{C} . If conflag=1, go to step 6; else go to step 7.

• **Step 6:** If there is no cables remaining, go to step 3, else go to step 8.

• **Step 7:** If this is the first time to add cables, save the indexes of the cables which cannot generate zonotope as Ininoofe; else add the indexes of the cables which cannot generate zonotope into Indexnofe. Compare Indexnofe with Ininoofe. If they are same, go to step 4; else go to step 8.

• **Step 8:** If Indexnofe is empty go to step 9; else go to step 3.

• **Step 9:** Add the Offset to the zonotope and exit the loop.

4 Simulations on a 24 DOFs MCDR platform

Cable-driven snake robots are one of the typical MCDRs. In

this section, we utilize the presented method on our customized 24 DOFs cable driven snake robot [3,8] to analysis its operational wrench capability. Figure 2(a) shows the schematic illustration of our snake robot with 12 sections, where each section has two DOFs, driven by three cables. In the simulations, the snake robot keeps tracking of a square trajectory, and the operational force capability is evaluated by the developed method at each pose, which is visualized in MATLAB as shown in Figure 2(b). All the parameters of the dynamics model are calculated and updated with the CASPR [10].

4.1 Simulation results

At a given pose ($\mathbf{q}=[0.1, 0.1, 0.1, \dots, 0.1, 0.1]^T$), the simulated snake arm and its end effector force zonotope are visualized in MATLAB. Detailed views such as 3D, XY, ZX, YZ views of the zonotope are shown in Figure 3. From the figures we can see there are many redundant vertices and faces which contribute little to the volume of capability zonotope. The number of cables added in each step (S_c) of the iterative is an important parameter, which effects the computation efficiency of the method. To study the time efficiency related to S_c , we generate the end effector force zonotope when the snake robot keeps tracking of a square with different S_c and record the time consuming at each pose.

The initial cable number is 6, and can be chosen randomly or not randomly. If the cables are chosen randomly, if rand is true, otherwise is false. The step number of cables are 1, 2, 3, 5, 6, and 10. The time consuming of each pose of the robot is recorded and shown in Figure 4. Detailed average time consuming of zonotope generation with different step cable numbers S_c are listed in Table 1. From Figure 4 and Table 1, we can see that the optimal step number of cables is 5.

4.2 Simplified zonotope representation

Another problem for the zonotope representation is there are too many redundant vertices and faces as shown in Figure 3, which has little contribution to the volume of the zonotope. We may mention that if a vertex has little contribution to the volume of the zonotope, it can be regarded as a redundant one. Thus, we can omit this vertex in the calculation for simplicity, which will be verified in the following simulation results. However, such redundant faces corresponding to the constraints of the robot make the post-process like manipulability optimization and motion planning difficult and inefficiency. Thus, we put forward a threshold to diminish the number of vertices faces. The detailed steps are as follows. The faces that contain a same point are found, and angles among these faces are calculated. If the maximum angle is less than the given face angle threshold, we omit this vertex

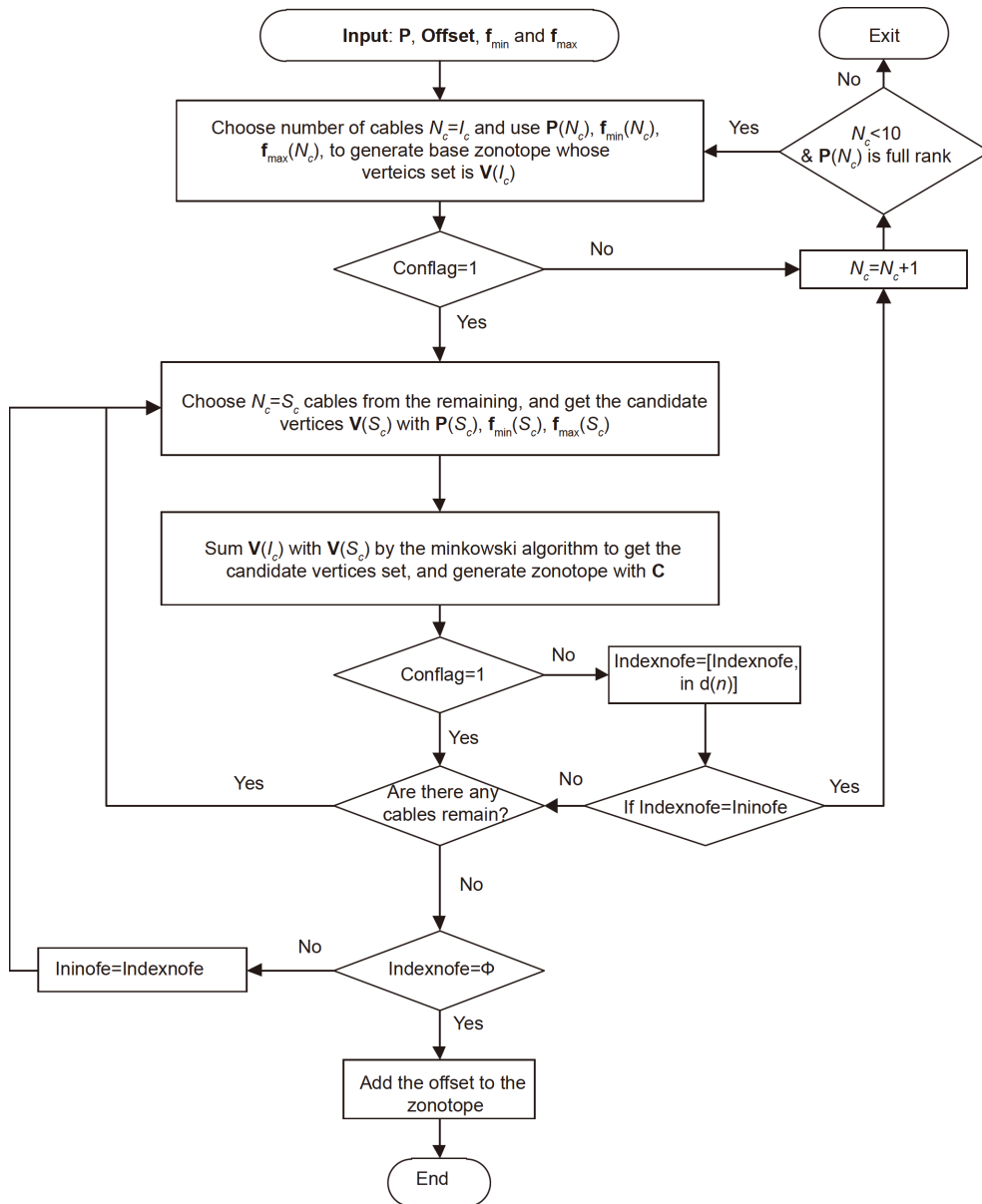


Figure 1 Flowchart of the iterative method for capability zonotope.

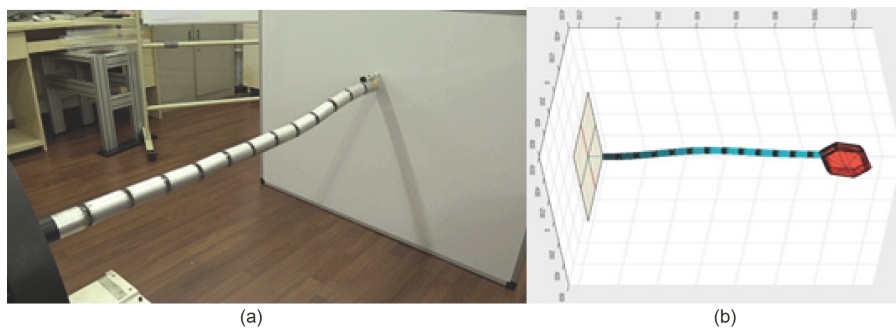


Figure 2 (Color online) The cable-driven snake robot and its capability analysis. (a) Cable-driven snake platform; (b) capability evaluation visualization.

for simplicity. According to this idea, the 3D, XY , ZX , YZ views of the simplified zonotope are shown in Figure 5. The number of vertices, faces and volume and calculation time of

the zonotope with respect to the face angle threshold are shown in Table 2. From Table 2, we can see that the simplified zonotope representation reduces the vertices and fa-

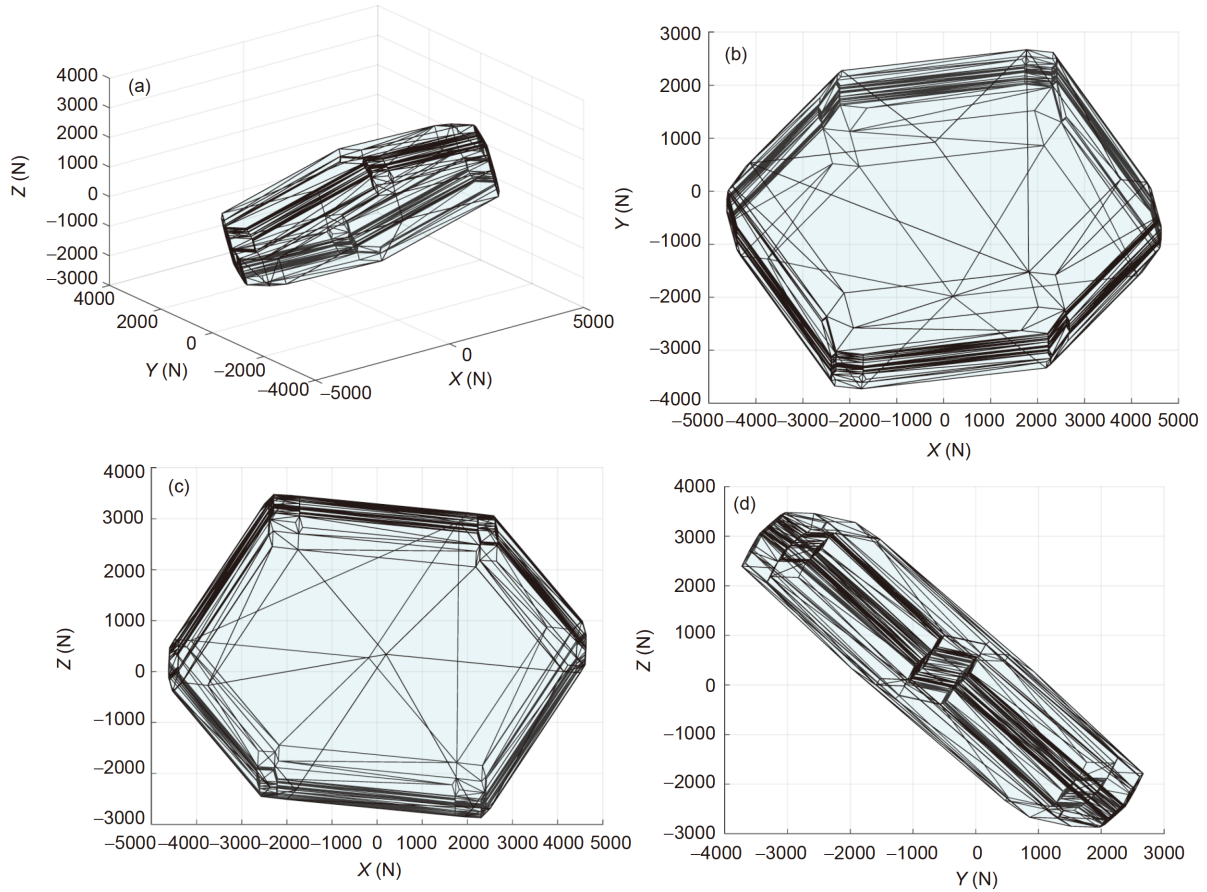


Figure 3 (Color online) Capability zonotope at the given pose. (a) 3D view; (b) XY view; (c) ZX view; (d) YZ view.

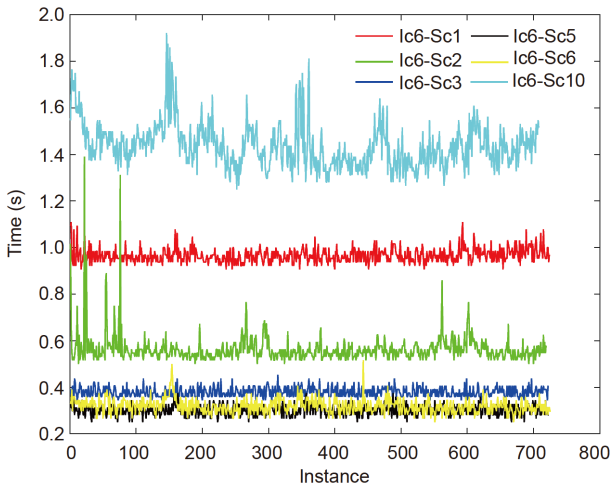


Figure 4 (Color online) Time consuming of end effector force zonotope at each pose when the robot keeps tracking of a square trajectory with different step cable numbers S_c .

ces from 1260 and 2516 to 88 and 172, respectively, with 3.3% volume loss.

4.3 Capability measurement

Capability indexes based on zonotopes are put forward to

Table 1 Average time consuming of zonotope generation

S_c	N-Random (s)	Random (s)
1	0.9663	0.6807
2	0.5638	0.3541
3	0.3792	0.2992
5	0.3009	0.2317
6	0.3188	0.2538
10	1.4372	1.0626

evaluate the payload capability of MCDRs. In this work, the zonotope volume, diameters and distances of capability ball and directions are utilized for the payload capability evaluation. The zonotope volume can acquire directly with the convhulln algorithm. The volume of the end effector force capability zonotope when the snake robot keeps tracking of the square trajectory are shown in [Figure 6](#).

(1) Capability ball metric

In some scenarios, payloads from all directions are needed to consider. For example, when a drill is attached to the end effector of the snake robot, and the end effector goes to drilling a hole, the force applied to the snake arm is from all directions. Thus, payload needs to be restricted in a ball.

For a reference point **gref**, the radius of the maximum ball

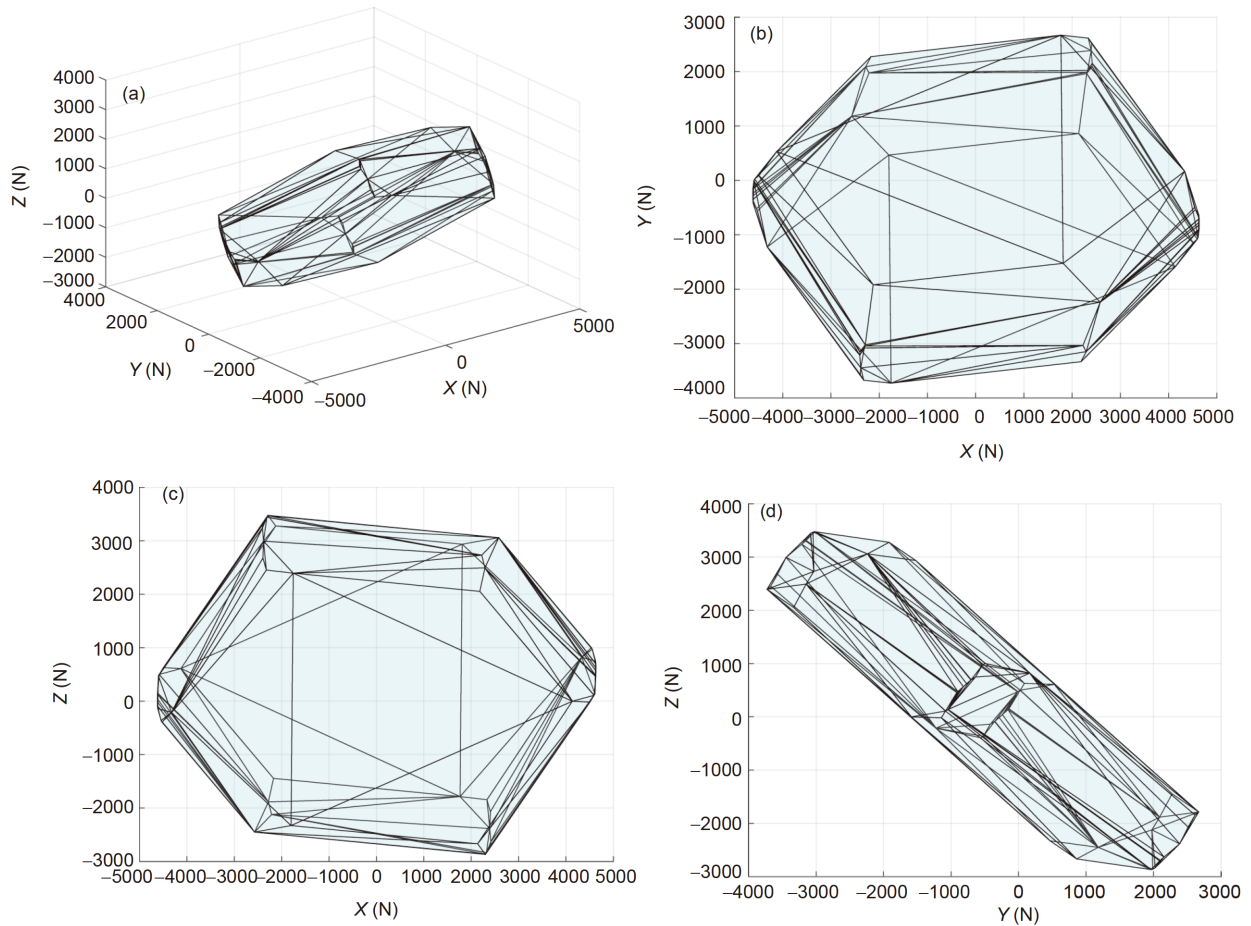


Figure 5 (Color online) 3D, XY, ZX, YZ views of the simplified zonotope. (a) 3D view; (b) XY view; (c) ZX view; (d) YZ view.

Table 2 Number of vertices, faces and volume and calculation time of the zonotope with respect to the face angle threshold

Angle threshold (degree)	Vertices	Faces	Volume ratio	Time (s)
0	1260	2516	1	2.8438
10	260	516	0.9978	1.7813
20	148	292	0.9932	1.7344
30	88	172	0.9671	1.7031

\mathbf{r} is defined as eq. (20) corresponding to the capability zonotope constraints. Given the reference point as the position which balanced gravity ($\mathbf{g}_{ref} = -\mathbf{G}$), the maximum ball radius of the end effector force capability zonotope when the snake robot keeps tracking of the square trajectory is shown in Figure 7.

$$\mathbf{r} = \min(\mathbf{b} - \mathbf{A}_c \mathbf{g}_{ref}). \quad (20)$$

(2) Capability direction metric

In some situations, the payload is in one direction, such as lifting objects. The direction of the payload is in the same direction with the gravity. Given the reference point and direction (\mathbf{g}_{ref} , $\mathbf{g}_{ref} \mathbf{D}_i$), the maximum payload is defined as

eq. (21) corresponding to the capability zonotope constraints. Given the reference point and the reference direction as the position which balanced gravity and the direction of the Z axis, respectively ($\mathbf{g}_{ref} = -\mathbf{G}$, $\mathbf{g}_{ref} \mathbf{D}_i = [0, 0, 1]^T$), the maximum capability direction distance of the end effector force capability zonotope when the snake robot keeps tracking of the square trajectory is shown in Figure 7.

$$\mathbf{D}_y = \min(\mathbf{y} = \mathbf{b} - \mathbf{A}_c \mathbf{g}_{ref}) / \mathbf{A}_c \mathbf{g}_{ref} \mathbf{D}_i. \quad (21)$$

5 Conclusion

In this paper, the operational space wrench and acceleration capability analysis of MCDRs are performed taking the actual actuation constraints of cables into consideration. According to the dynamics of the MCDRs, the hypercube generated by all cable forces can be projected to the joint space or the operational space to form wrench and acceleration capability zonotopes. Using the projection of the force hypercube vertices, a zonotope can be numerically found. However with increasing cables, the number of points

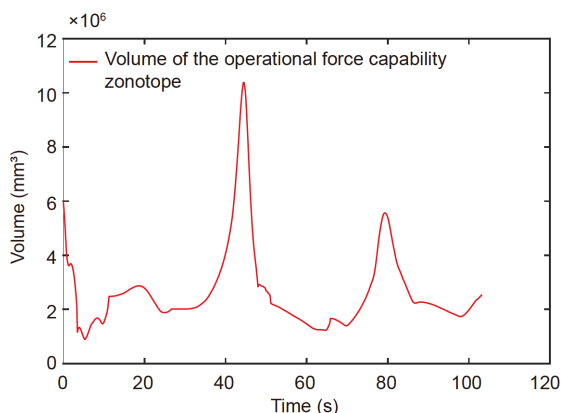


Figure 6 (Color online) Volume of the end effector force capability zonotope when the snake robot keeps tracking of the square trajectory.

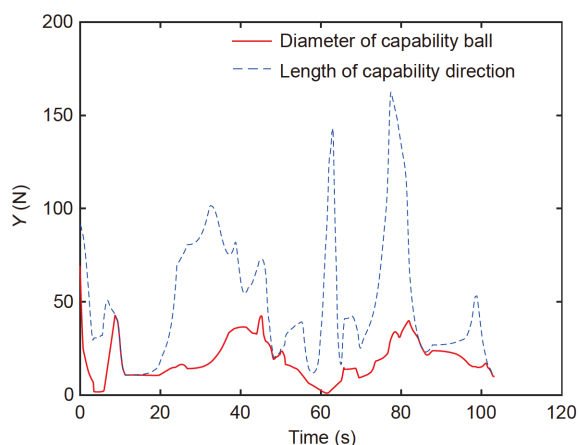


Figure 7 (Color online) Maximum ball radius and maximum direction distance of the end effector force capability zonotope when the snake robot keeps tracking of the square trajectory.

to be processed grows exponentially which is computationally infeasible. An efficient iterative method is proposed to acquire operational space acceleration and wrench capability of MCDRs with little memory requirement. In addition, large numbers of vertices and faces of the capability zonotopes are generated due to the hyper-redundancy of actuators, which has little contribution to the volume of the zonotope and makes the computation cumbersome of post-processing like manipulability optimization and motion planning. Therefore, a simplified zonotope capability representation is developed to prune large vertices and faces with little volume loss.

Simulations on our 24 DOFs cable-driven snake robot are performed to verify the effectiveness of the presented method. Simulation results show the normal operational wrench capability evaluation needs 18432 GB ROM, while the iterative method can easily solve this problem with a few MB ROM. The simplified representation reduces the vertices and faces from 1260 and 2516 to 88 and 172, respectively, with 3.3% volume loss. Finally, capability indexes such as

volume, diameters and distances of capability ball and directions based on capability zonotopes are put forward to evaluate the payload capability of the robot when keeping tracking of a square trajectory, which well verifies the presented method.

This work was supported by the China National Key R&D Program (Grant No. 2019YFB1311204), and the Shanghai Jiao Tong University Scientific and Technological Innovation Funds.

- 1 Axinte D, Dong X, Palmer D, et al. MiRoR—Miniaturised robotic systems for holistic *in-situ* repair and maintenance works in restrained and hazardous environments. *IEEE/ASME Trans Mechatron*, 2018, 23: 978–981
- 2 Buckingham R O, Graham A C. Dexterous manipulators for nuclear inspection and maintenance—Case study. In: 2010 1st International Conference on Applied Robotics for the Power Industry. Montreal, 2010. 1–6
- 3 Tang L, Zhu L M, Zhu X Y, et al. Confined spaces path following for cable-driven snake robots with prediction lookup and interpolation algorithms. *Sci China Tech Sci*, 2020, 63: 255–264
- 4 Gagliardini L, Caro S, Gouttefarde M, et al. A reconfiguration strategy for reconfigurable cable-driven parallel robots. In: 2015 IEEE International Conference on Robotics and Automation (ICRA). Seattle: IEEE, 2015. 1613–1620
- 5 Lamaury J, Gouttefarde M. Control of a large redundantly actuated cable-suspended parallel robot. In: 2013 IEEE International Conference on Robotics and Automation. Karlsruhe: IEEE, 2013. 4659–4664
- 6 Kawamura S, Choe W, Tanaka S, et al. Development of an ultrahigh speed robot FALCON using wire drive system. In: Proceedings of 1995 IEEE International Conference on Robotics and Automation. Nagoya: IEEE, 1995. 215–220
- 7 Mao Y, Agrawal S K. Transition from mechanical arm to human arm with CAREX: A cable driven ARm EXoskeleton (CAREX) for neural rehabilitation. In: 2012 IEEE International Conference on Robotics and Automation. St Paul, MN: IEEE, 2012. 2457–2462
- 8 Tang L, Wang J, Zheng Y, et al. Design of a cable-driven hyper-redundant robot with experimental validation. *Int J Adv Robotic Syst*, 2017, 14: doi: 10.1177/1729881417734458
- 9 Williams R L, Albus J S, Bostelman R V. 3D cable-based Cartesian metrology system. *J Robotic Syst*, 2004, 21: 237–257
- 10 Lau D, Eden J, Tan Y, et al. CASPR: A comprehensive cable-robot analysis and simulation platform for the research of cable-driven parallel robots. In: 2016 IEEE/RSJ International Conference on Intelligent Robots and Systems (IROS). Daejeon, 2016. 3004–3011
- 11 Oh S R, Ryu J C, Agrawal S K. Dynamics and control of a helicopter carrying a payload using a cable-suspended robot. *J Mech Des*, 2006, 128: 1113–1121
- 12 Bosscher P, Williams II R L, Bryson L S, et al. Cable-suspended robotic contour crafting system. *Autom Constr*, 2007, 17: 45–55
- 13 Tadokoro S, Matsushima T, Murao Y, et al. A parallel cable-driven motion base for virtual acceleration. In: Proceedings 2001 IEEE/RSJ International Conference on Intelligent Robots and Systems. Expanding the Societal Role of Robotics in the the Next Millennium (Cat. No. 01CH37180). Maui, 2001. 1700–1705
- 14 Buckingham R, Chitrakaran V, Conkie R, et al. Snake-arm robots: A new approach to aircraft assembly. SAE Technical Paper 2007-01-3870
- 15 Tang L, Huang J, Zhu L M, et al. Path tracking of a cable-driven snake robot with a two-level motion planning method. *IEEE/ASME Trans Mechatron*, 2019, 24: 935–946
- 16 Li Z, Wu L, Ren H, et al. Kinematic comparison of surgical tendon-driven manipulators and concentric tube manipulators. *Mechanism*

- [Machine Theor](#), 2017, 107: 148–165
- 17 Pham C B, Yeo S H, Yang G, et al. Force-closure workspace analysis of cable-driven parallel mechanisms. [Mechanism Machine Theor](#), 2006, 41: 53–69
 - 18 Bouchard S, Gosselin C, Moore B. On the ability of a cable-driven robot to generate a prescribed set of wrenches. [J Mech Robotics](#), 2009, 2: 011010
 - 19 Eden J, Lau D, Tan Y, et al. Available acceleration set for the study of motion capabilities for cable-driven robots. [Mechanism Machine Theor](#), 2016, 105: 320–336
 - 20 Bosscher P, Riechel A T, Ebert-Uphoff I. Wrench-feasible workspace generation for cable-driven robots. [IEEE Trans Robot](#), 2006, 22: 890–902
 - 21 Hassan M, Khajepour A. Analysis of bounded cable tensions in cable-actuated parallel manipulators. [IEEE Trans Robot](#), 2011, 27: 891–900
 - 22 Yoshikawa T. Manipulability of robotic mechanisms. [Int J Robotics Res](#), 1985, 4: 3–9
 - 23 Mustafa S K, Agrawal S K. On the force-closure analysis of n -DOF cable-driven open chains based on reciprocal screw theory. [IEEE Trans Robot](#), 2012, 28: 22–31
 - 24 Rezazadeh S, Behzadipour S. Workspace analysis of multibody cable-driven mechanisms. [J Mech Robotics](#), 2011, 3: 021005
 - 25 Grünbaum B. *Convex Polytopes*. 2nd ed. New York: Springer Verlag, 2003
 - 26 de Berg M. *Computational Geometry: Algorithms and Applications*. New York: Springer, 2000
 - 27 Lau D, Oetomo D, Halgamuge S K. Inverse dynamics of multilink cable-driven manipulators with the consideration of joint interaction forces and moments. [IEEE Trans Robot](#), 2015, 31: 479–488
 - 28 Lau D, Oetomo D, Halgamuge S K. Generalized modeling of multi-link cable-driven manipulators with arbitrary routing using the cable-routing matrix. [IEEE Trans Robot](#), 2013, 29: 1102–1113
 - 29 Taghirad H D, Bedoustani Y B. An analytic-iterative redundancy resolution scheme for cable-driven redundant parallel manipulators. [IEEE Trans Robot](#), 2011, 27: 1137–1143
 - 30 Lim W B, Yeo S H, Yang G. Optimization of tension distribution for cable-driven manipulators using tension-level index. [IEEE/ASME Trans Mechatron](#), 2014, 19: 676–683